Overshoot pathways reshape unequal heatwave health burdens across generations

Author:

Ayizhati Tuerxun[1,2], Hongjin Tian[3], Siying Zhu[2], Yue He[4], Yongye Jiang[3], Yuqin Lai[3], Guolong Chen[3], Yuxin Huang[1,2], Runmei Ma[5], Xiaoqian Jia[1], Zhenyu Zhang[4,6], Bin Wang[1,3], Bo Fu[1,4,*], Bengang Li[3,4]

1. Institute of Reproductive and Child Health/National Health Commission Key Laboratory of Reproductive Health, School of Public Health, Peking University, Beijing, China
2. Department of Epidemiology and Biostatistics, School of Public Health, Peking University, Beijing, China
3. College of Urban and Environmental Sciences, Peking University, Beijing, China.
4. Institute of Carbon Neutrality, Peking University, Beijing, China.
5. National Institute of Environmental Health, Chinese Center for Disease Control and Prevention, Beijing, China
6. Institute for Global Health and Development, Peking University School of Public Health, Beijing, China

*. Corresponding author (pkufubo@pku.edu.cn).

Data Sources and Model Selection

Daily maximum temperature (T_{max}) data were localized from the Coupled Model Intercomparison Project Phase 6 (CMIP6). To ensure a robust multi-model ensemble (MME), we selected a suite of Global Climate Models (GCMs) based on the availability of daily outputs for all four target scenarios: SSP1-2.6, SSP2-4.5, SSP5-8.5, and SSP5-3.4-overshoot (Supplementary Table 1).All models provide continuous daily simulations covering the historical period (1850–2014) and future projections (2015–2100). To account for varying spatial resolutions across different modeling groups, all GCM outputs were bilinearly interpolated to a common horizontal grid before hazard calculation.

Supplementary Table 1. Characteristics of selected CMIP6 models and experiment configurations for different climate scenarios.

Model Name	Variant Label	Institution /Group	Country	Scenarios Used	Projection Period
ACCESS-CM2	r1i1p1f1	CSIRO-ARCCSS	Australia	126, 245, 585, 534os	2015-2100
ACCESS-ESM1-5	r1i1p1f1	CSIRO	Australia	534os	2041-2100
AWI-CM-1-1-MR	r1i1p1f1	AWI	Germany	126, 245, 585	2015-2100
CanESM5	r1i1p1f1	CCCma	Canada	534os	2040-2300
CMCC-ESM2	r1i1p1f1	CMCC	Italy	534os	2015-2100
CNRM-ESM2-1	r1i1p1f2	CNRM-CERFACS	France	534os	2015-2300
EC-Earth3-Veg-LR	r1i1p1f1	EC-Earth	Europe	126, 245, 585	2015-2100
FGOALS-g3	r1i1p1f1	CAS	China	534os	2015-2100
INM-CM5-0	r1i1p1f1	INM	Russia	126, 245, 585	2015-2100
IPSL-CM6A-LR	r1i1p1f1	IPSL	France	534os	2040-2300
MIROC6	r1i1p1f1	MIROC	Japan	126, 245, 585, 534os	2015-2100
MIROC-ES2L	r1i1p1f2	MIROC	Japan	534os	2015-2200
MRI-ESM2-0	r1i1p1f1	MRI	Japan	534os	2040-2200
UKESM1-0-LL	r4i1p1f2	MOHC	UK	534os	2040-2100

Institution abbreviations: AWI, Alfred Wegener Institute, Helmholtz Centre for Polar and Marine Research; **CAS**, Chinese Academy of Sciences (Institute of Atmospheric Physics); **CCCma**, Canadian Centre for Climate Modelling and Analysis; **CMCC**, Fondazione Centro Euro-Mediterraneo sui Cambiamenti Climatici; **CNRM-CERFACS**, Centre National de Recherches Météorologiques - Centre Européen de Recherche et de Formation Avancée en Calcul Scientifique; **CSIRO**, Commonwealth Scientific and Industrial Research Organisation; **CSIRO-ARCCSS**, Commonwealth Scientific and Industrial Research Organisation - Australian Research Council Centre of Excellence for Climate System Science; **EC-Earth**, EC-Earth Consortium; **INM**, Institute for Numerical Mathematics of the Russian Academy of Sciences; **IPSL**, Institut Pierre-Simon Laplace; **MIROC**, Japan Agency for Marine-Earth Science and Technology, University of Tokyo, and National Institute for Environmental Studies; **MOHC**, Met Office Hadley Centre; **MRI**, Meteorological Research Institute. All models provide daily T_{max}

projections for the historical period (1850 – 2014).

Calculation of Heatwave-related Health Risk Weights

These weights are derived from the Global Burden of Disease (GBD) study, specifically utilizing mortality rates attributable to non-optimal temperatures (Supplementary Table 2). To ensure the stability and representativeness of the vulnerability profile, we calculated the global average mortality rates for the period 2019-2023. These rates serve as a proxy for the intrinsic physiological susceptibility of different life stages. This normalization ensures that the resulting health risk index remains dimensionless, facilitating a relative comparison of the cumulative thermal burden across different birth cohorts and geographical regions.

Supplementary Table 2. Normalized vulnerability weights across different age groups derived from the Global Burden of Disease (GBD) study.

Age Group	Corresponding Life Stage	Average Mortality Rate (per 100,000)	Normalized Vulnerability Weight
0-4	Childhood	0.142	0.029
5-9	Childhood	0.044	0.009
10-19	Childhood	0.070	0.014
20-54	Adulthood	0.520	0.107
55-59	Adulthood	1.422	0.294
60-75	Aged	2.642	0.546

Results of Generational Heatwave Exposure and Health Risk across Regions

To provide a comprehensive assessment of generational heatwave inequities across diverse geographical contexts, we extended our analysis from the three representative regions discussed in the main text to all 21 Global Burden of Disease (GBD) regions.

The geographical classification and boundaries of these regions are visualized in Supplementary Figure 1, while their corresponding standardized abbreviations are detailed in Supplementary Table 3. The subsequent Supplementary Figures 2-22 provide the localized results for generational heatwave exposure and health risk in each region, illustrating the universal nature of the observed temporal shifts.

Across all 21 Regions, a consistent "peak-and-decline" trajectory is observed in both lifetime heatwave exposure (blue) and age-weighted health risk (red) under the temperature overshoot scenario(Supplementary Figs. 2–22). Despite regional variations in absolute intensity, a universal temporal decoupling persists: the generation facing the maximum cumulative exposure (hazard-peak) typically lags 10–35 years behind the generation facing the highest lifetime health risk (risk-peak). This systemic gap highlights that while younger cohorts bear the brunt of intensifying physical hazards, mid-century cohorts often experience a higher integrated health burden due to the synchronization of peak heatwave intensity with their high-vulnerability life stages.

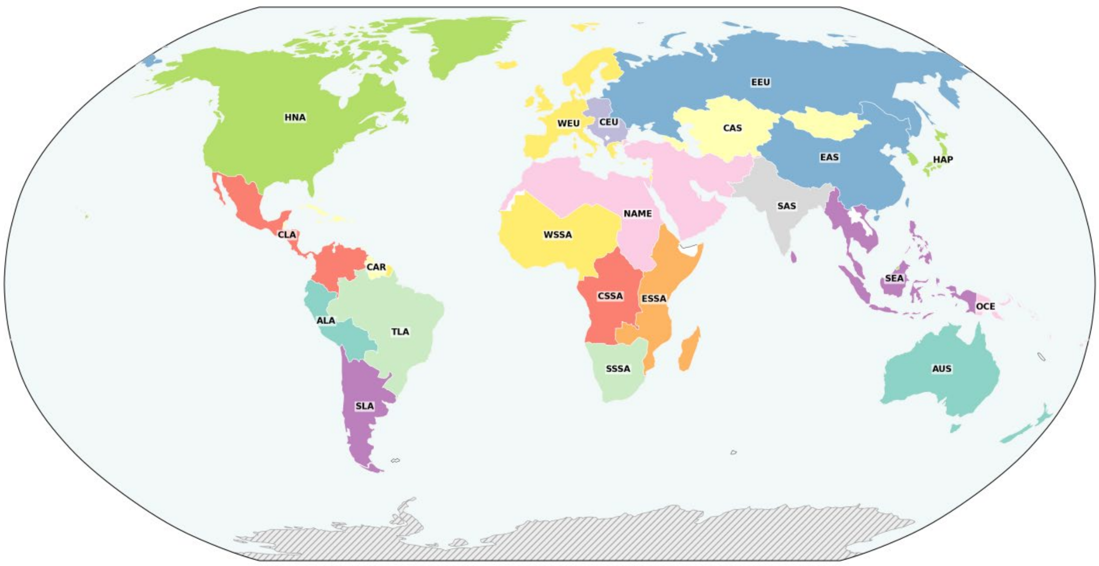

Supplementary Figure 1. Geographical classification of the 21 regions.

Supplementary Table 3. Standardized abbreviations for the 21 regions.

GBD Region	Abbreviation
Andean Latin America	ALA

Australasia	AUS
Caribbean	CAR
Central Asia	CAS
Central Europe	CEU
Central Latin America	CLA
Central Sub-Saharan Africa	CSSA
East Asia	EAS
Eastern Europe	EEU
Eastern Sub-Saharan Africa	ESSA
High-income Asia Pacific	HAP
High-income North America	HNA
North Africa and Middle East	NAME
Oceania	OCE
South Asia	SAS
Southeast Asia	SEA
Southern Latin America	SLA
Southern Sub-Saharan Africa	SSSA
Tropical Latin America	TLA
Western Europe	WEU
Western Sub-Saharan Africa	WSSA

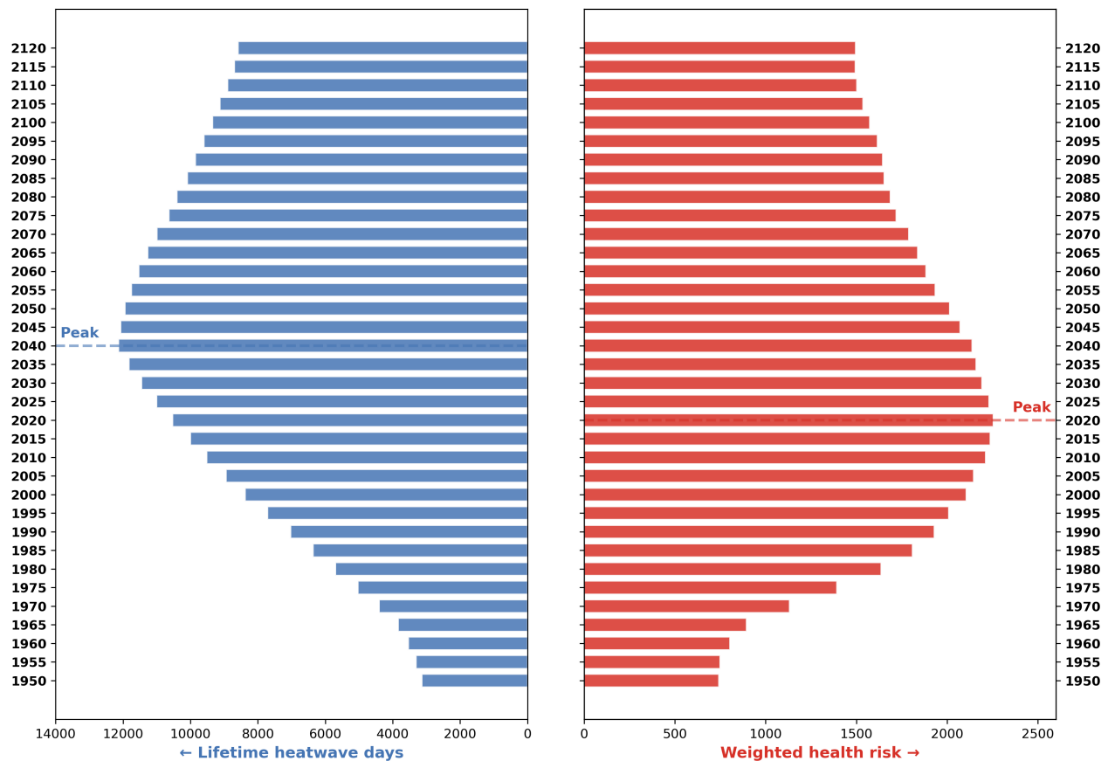

Supplementary Figure 2. Cohort profiles of lifetime heatwave exposure and health risk for Andean Latin America. Blue and red lines represent the multi-model mean of lifetime cumulative heatwave exposure and age-weighted health risk, respectively, across birth cohorts under the overshoot pathway. Similar to the representative regions in the main text (Fig. 4d-f), a temporal shift between peak exposure and peak risk is observed, driven by the interplay between intensifying heatwave hazards and age-specific physiological vulnerabilities. For a detailed definition of the dimensionless health risk index and its underlying weighting functions, see Methods and Fig. 4 legend.

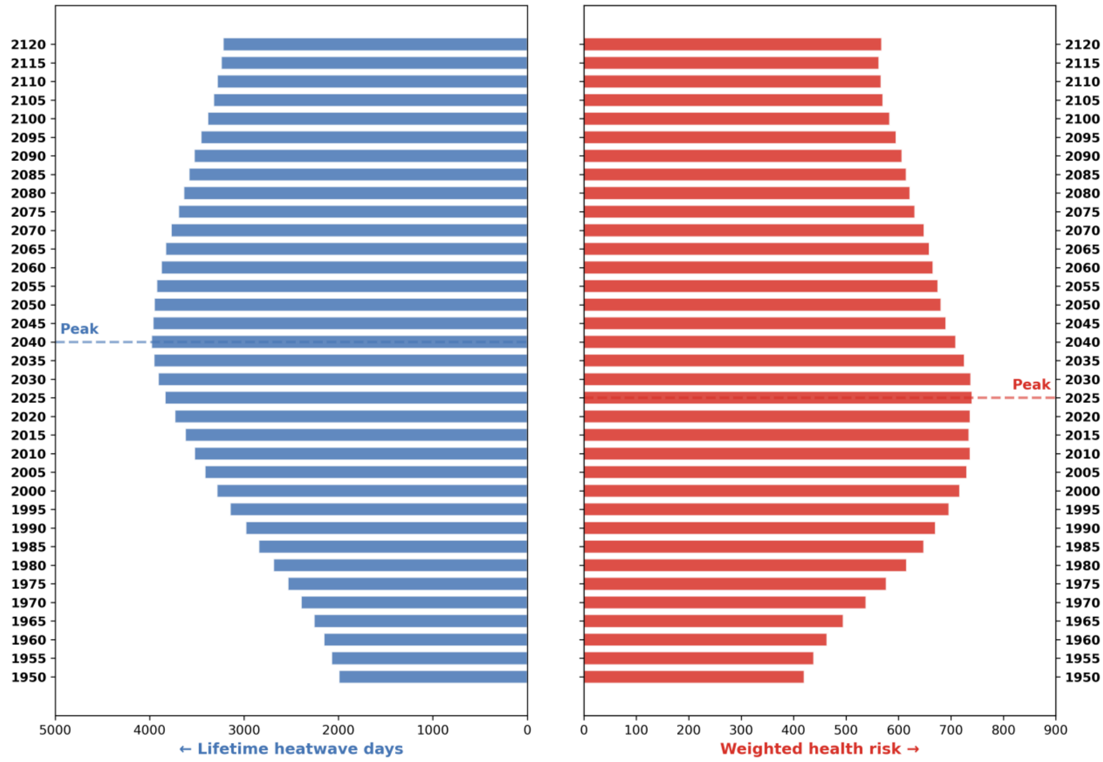

Supplementary Figure 3. Cohort profiles of lifetime heatwave exposure and health risk for Australasia. In Australasia, the generation with the highest lifetime heatwave exposure is born in 2040, but the highest health risk is observed in those born 15 years earlier, in 2025.

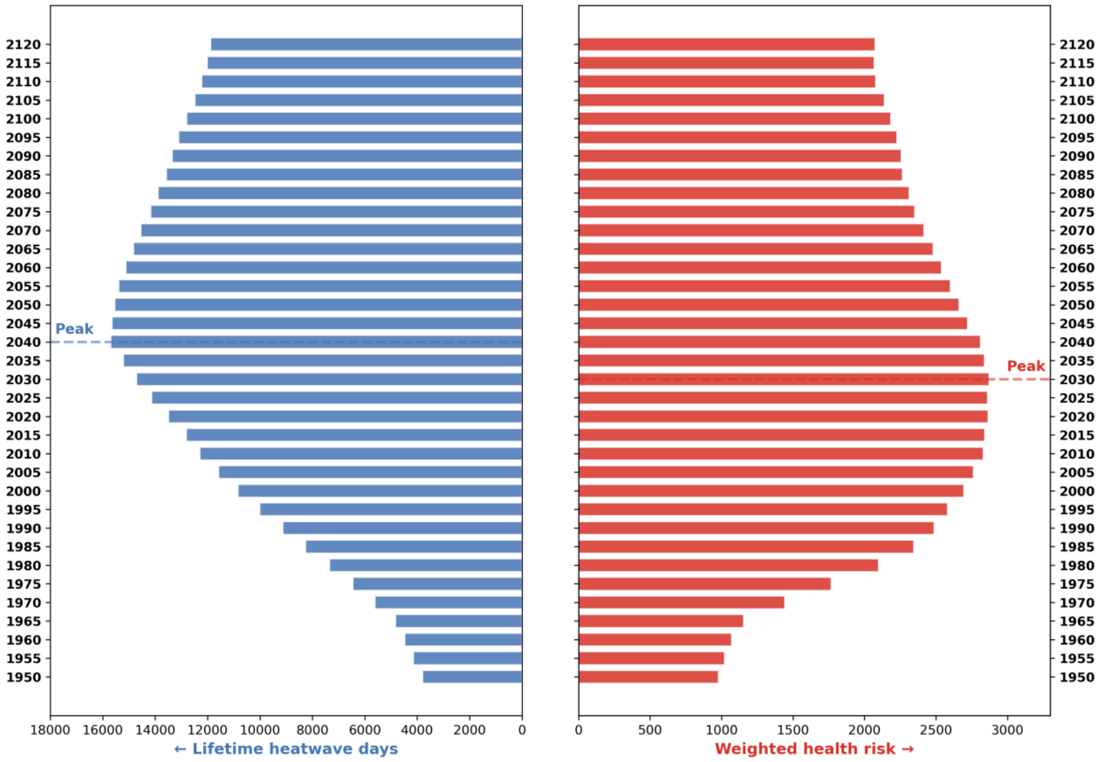

Supplementary Figure 4. Cohort profiles of lifetime heatwave exposure and health risk for Caribbean. The Caribbean exhibits a 10-year offset between its most exposed generation (2040 cohort) and its most at-risk generation (2030 cohort), the shortest gap observed among the regions.

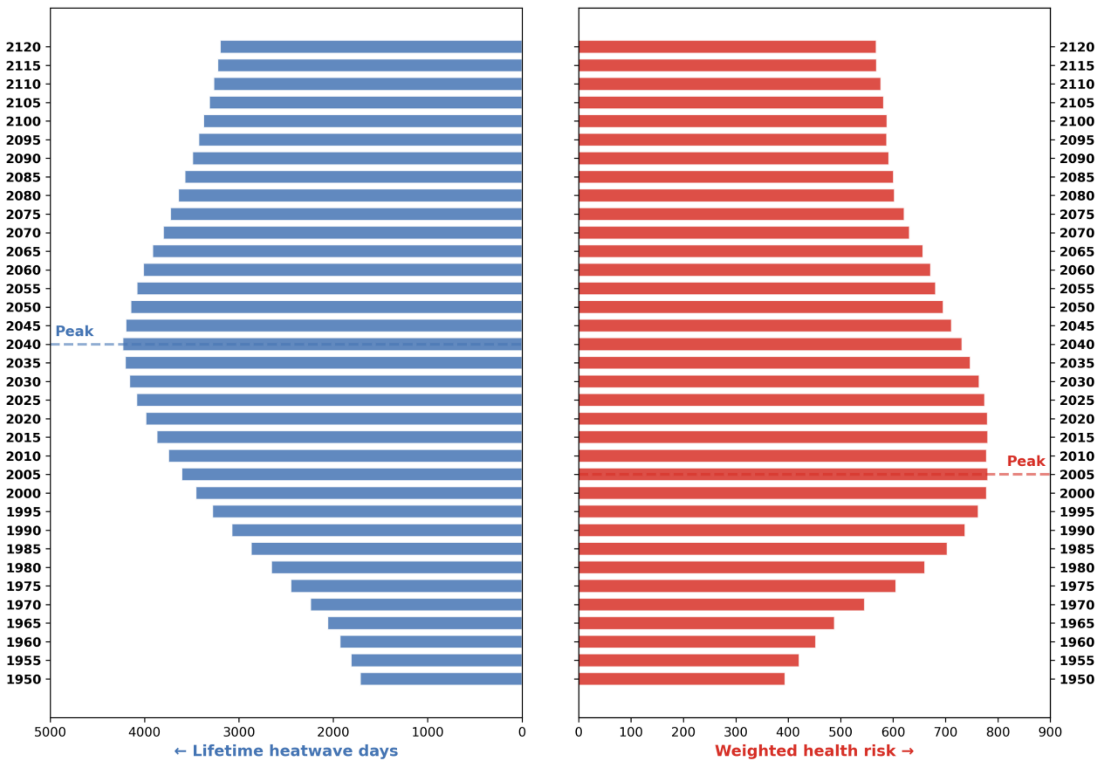

Supplementary Figure 5. Cohort profiles of lifetime heatwave exposure and health risk for Central Asia. For Central Asia, a substantial 35-year lead is observed in the health risk peak

(2005 cohort) relative to the exposure peak (2040 cohort), one of the largest temporal shifts across all regions.

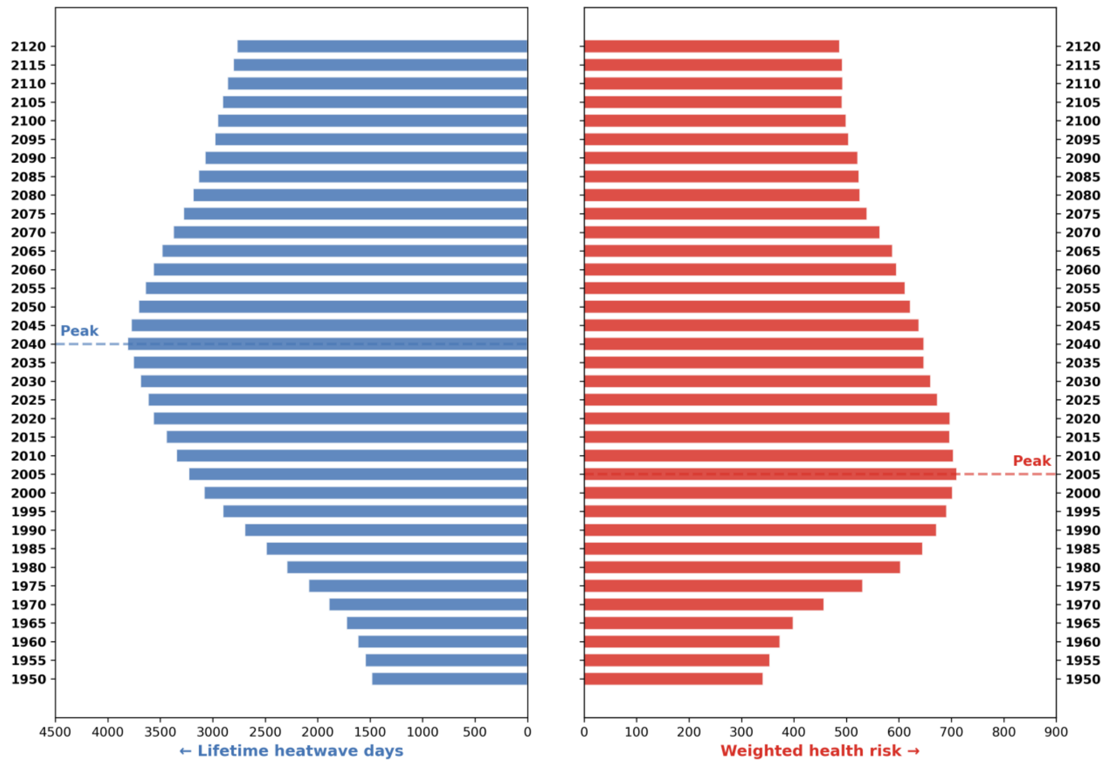

Supplementary Figure 6. Cohort profiles of lifetime heatwave exposure and health risk for Central Europe. A pronounced mismatch is evident in Central Europe: while lifetime exposure peaks for the 2040 cohort, the cumulative health risk reaches its maximum 35 years earlier (2005 cohort), reflecting a significant lead time in risk accumulation.

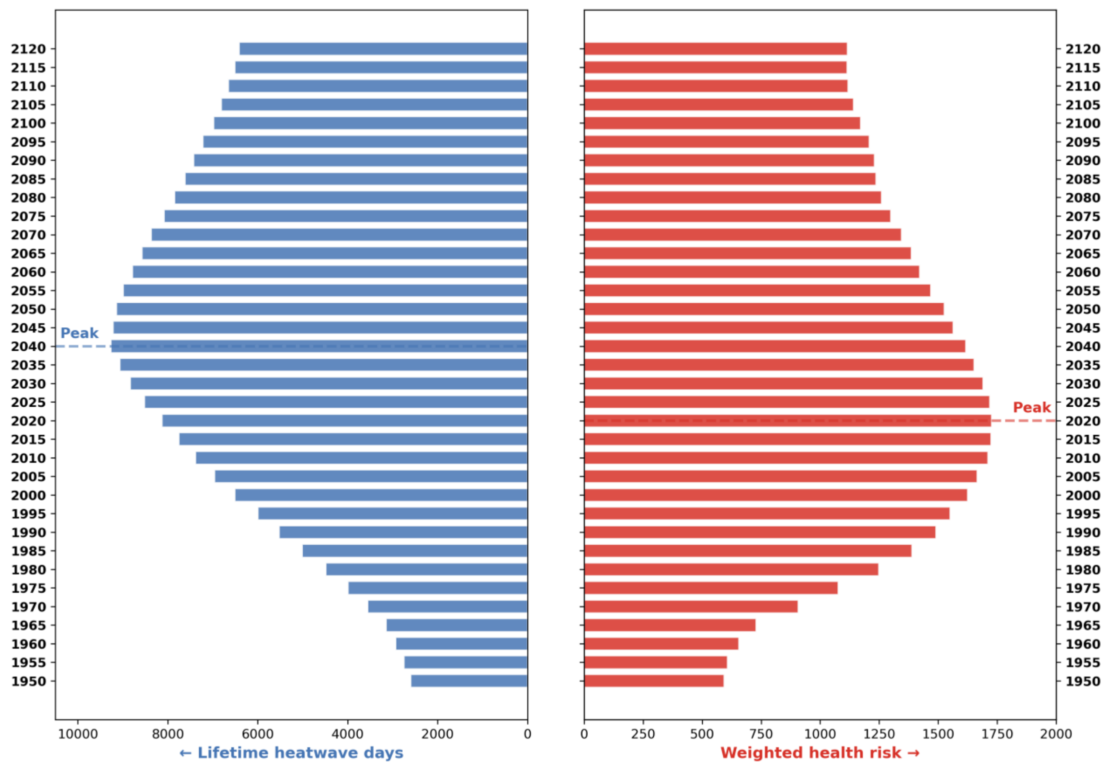

Supplementary Figure 7. Cohort profiles of lifetime heatwave exposure and health risk for Central Latin America. In Central Latin America, the peak of lifetime health risk (2020 cohort) precedes the peak of physical exposure (2040 cohort) by two decades.

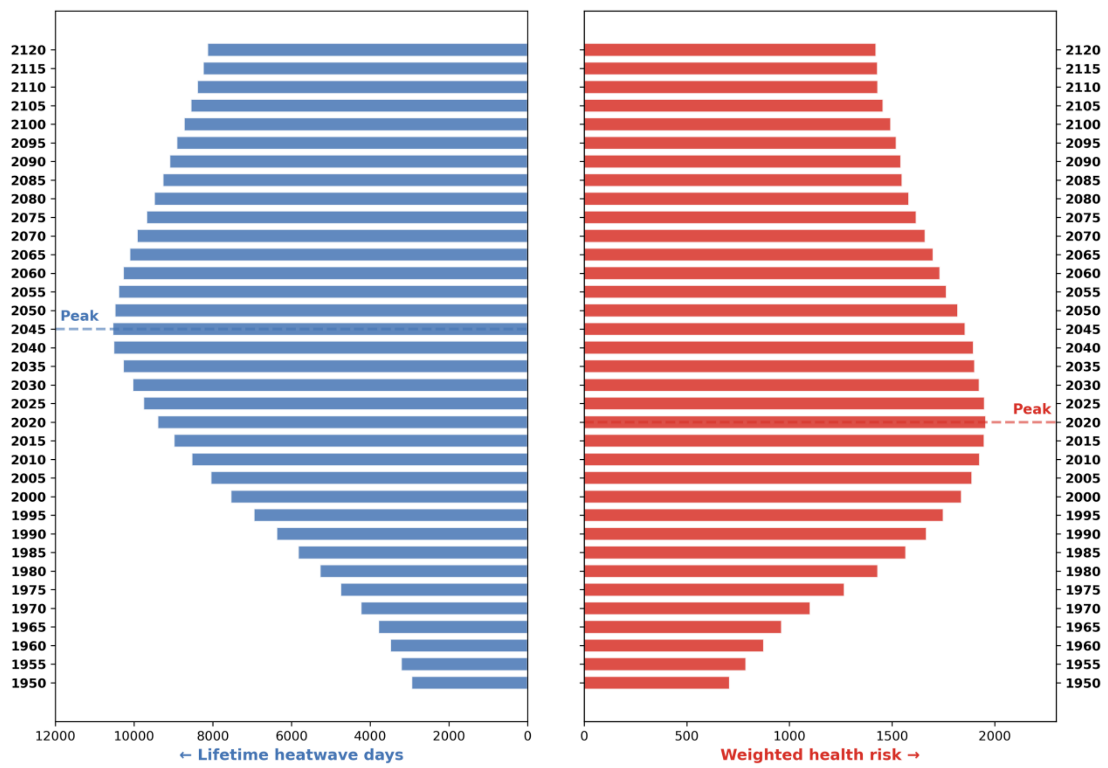

Supplementary Figure 8. Cohort profiles of lifetime heatwave exposure and health risk for Central Sub-Saharan Africa. In Central Sub-Saharan Africa, the generation with the highest lifetime heatwave exposure is born in 2045, but the highest health risk is observed in those born 25 years earlier, in 2020.

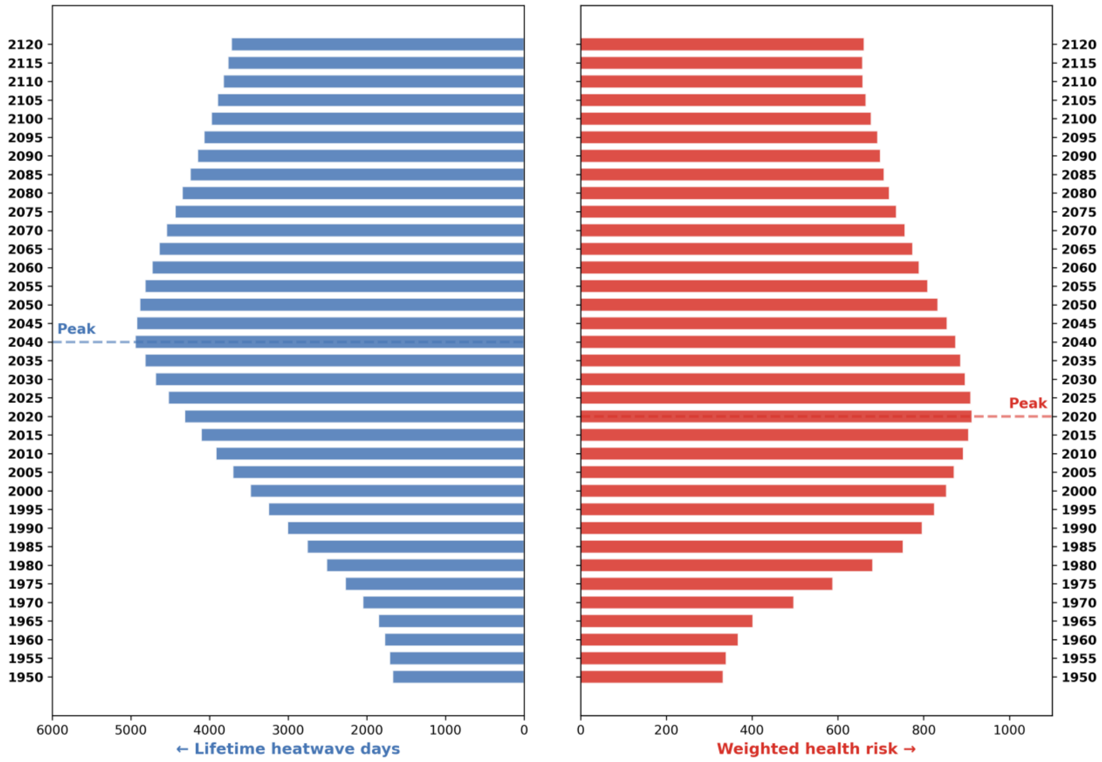

Supplementary Figure 9. Cohort profiles of lifetime heatwave exposure and health risk for East Asia. In East Asia, the peak of lifetime health risk (2020 cohort) precedes the peak of physical exposure (2040 cohort) by two decades.

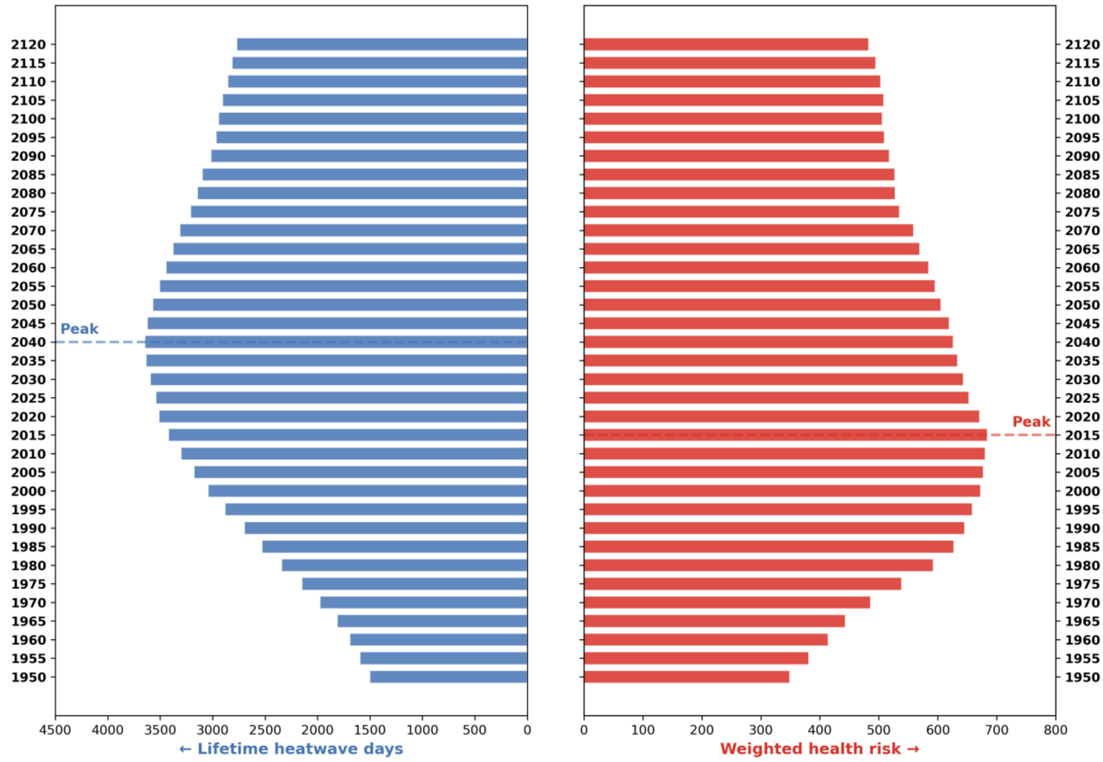

Supplementary Figure 10. Cohort profiles of lifetime heatwave exposure and health risk for Eastern Europe. In Eastern Europe, the generation with the highest lifetime heatwave exposure is born in 2040, but the highest health risk is observed in those born 25 years earlier, in 2015.

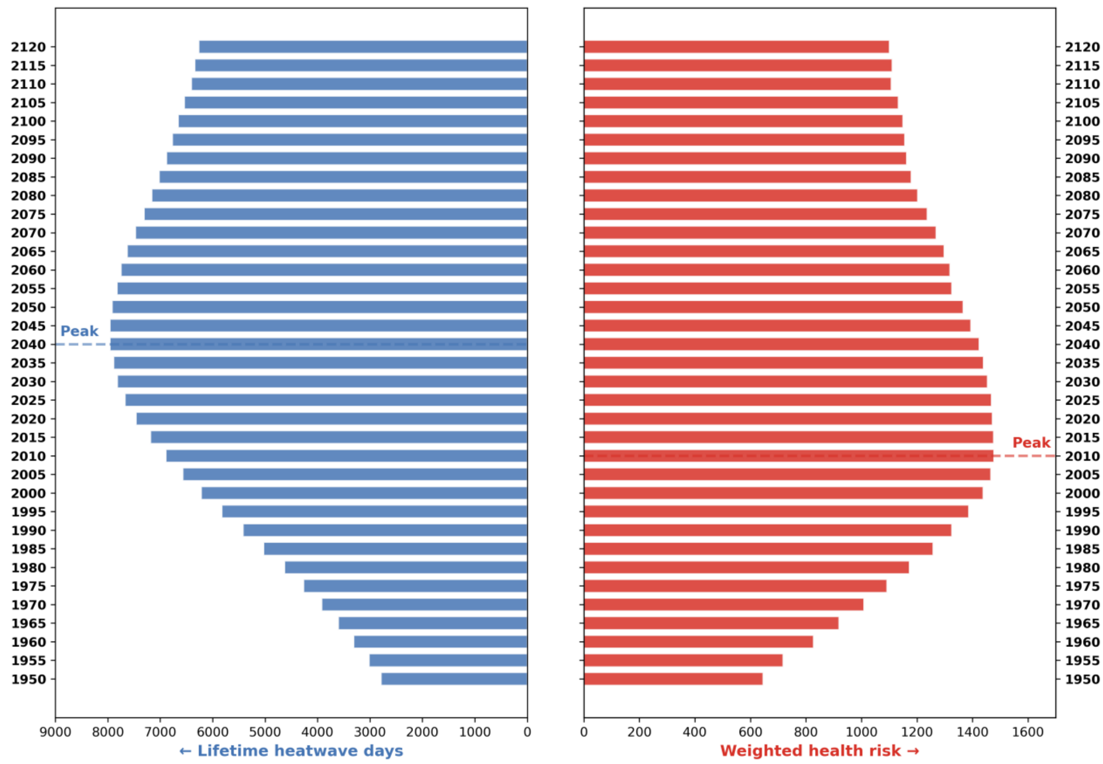

Supplementary Figure 11. Cohort profiles of lifetime heatwave exposure and health risk for Eastern Sub-Saharan Africa. A pronounced mismatch is evident in Eastern Sub-Saharan Africa:

while lifetime exposure peaks for the 2040 cohort, the cumulative health risk reaches its maximum 30 years earlier (2010 cohort), reflecting a significant lead time in risk accumulation.

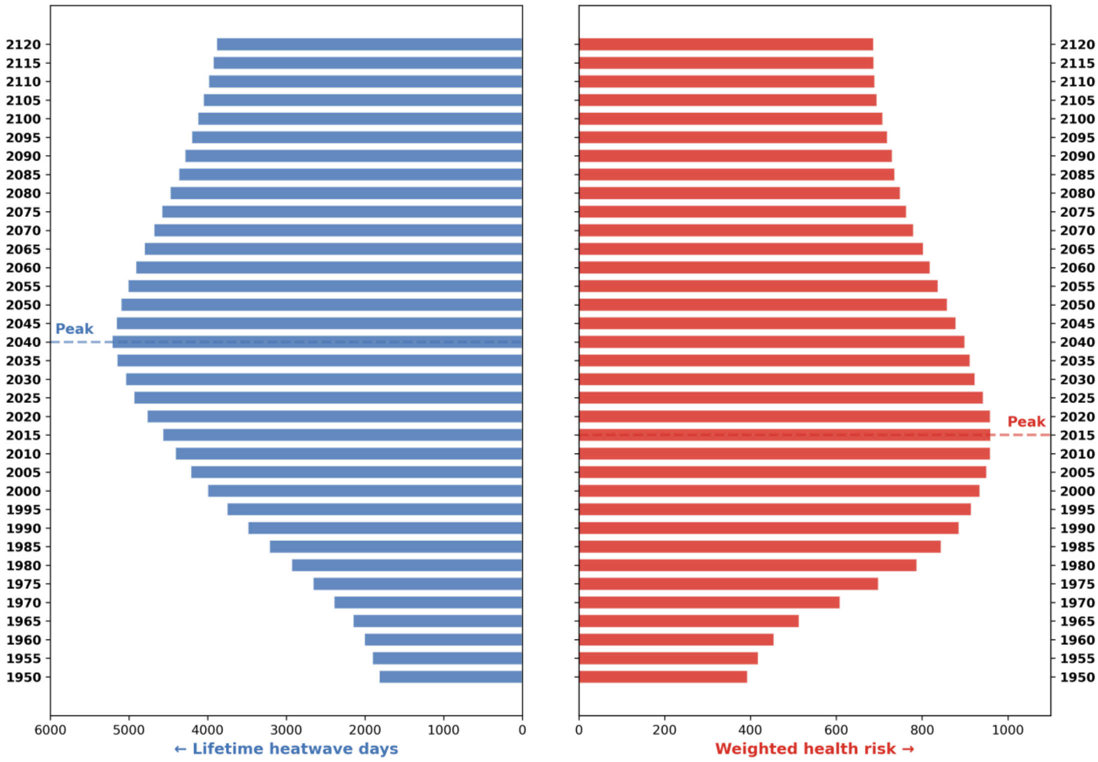

Supplementary Figure 12. Cohort profiles of lifetime heatwave exposure and health risk for High-income Asia Pacific. In High-income Asia Pacific, the generation with the highest lifetime heatwave exposure is born in 2040, but the highest health risk is observed in those born 25 years earlier, in 2015.

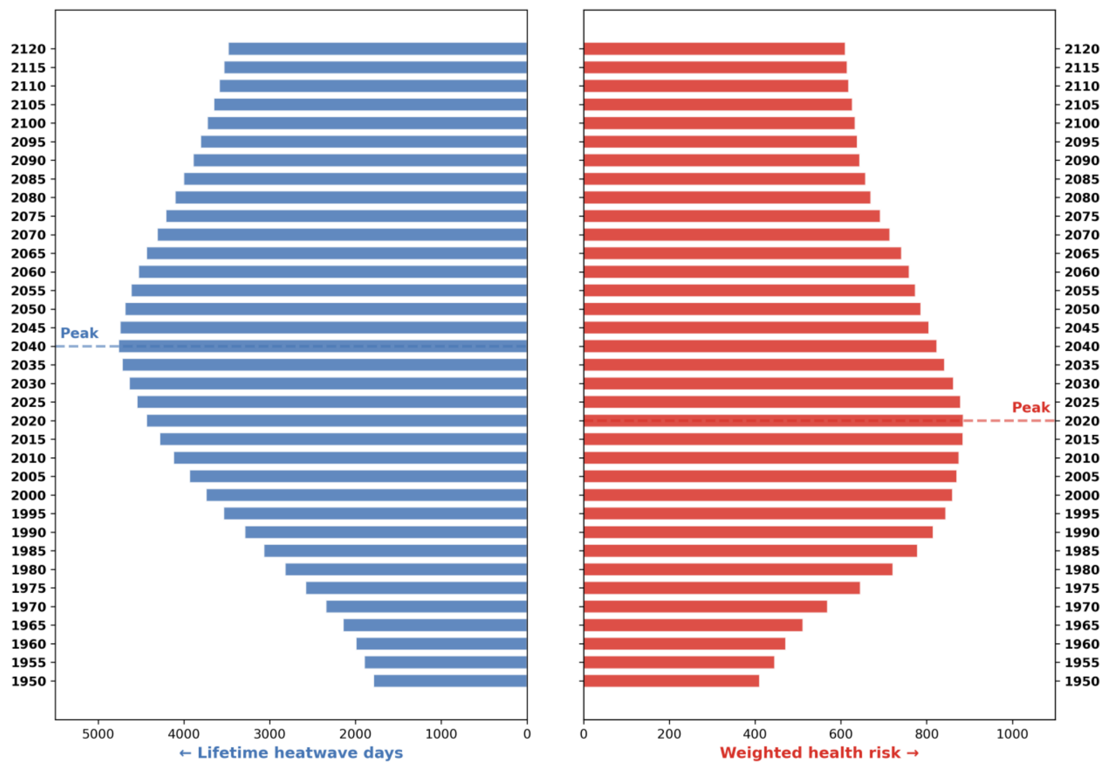

Supplementary Figure 13. Cohort profiles of lifetime heatwave exposure and health risk for High-income North America. In High-income North America, the generation with the highest lifetime heatwave exposure is born in 2040, but the highest health risk is observed in those born 20 years earlier, in 2020.

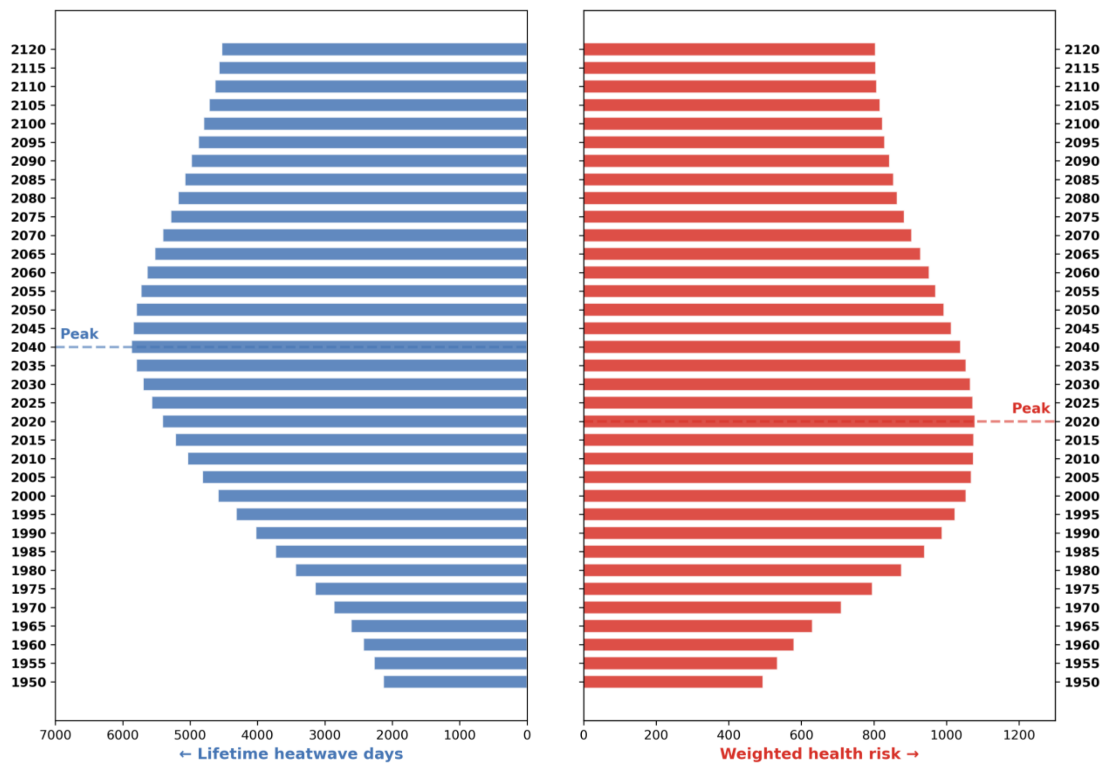

Supplementary Figure 14. Cohort profiles of lifetime heatwave exposure and health risk for

North Africa and Middle East. In North Africa and Middle East, the peak of lifetime health risk (2020 cohort) precedes the peak of physical exposure (2040 cohort) by two decades.

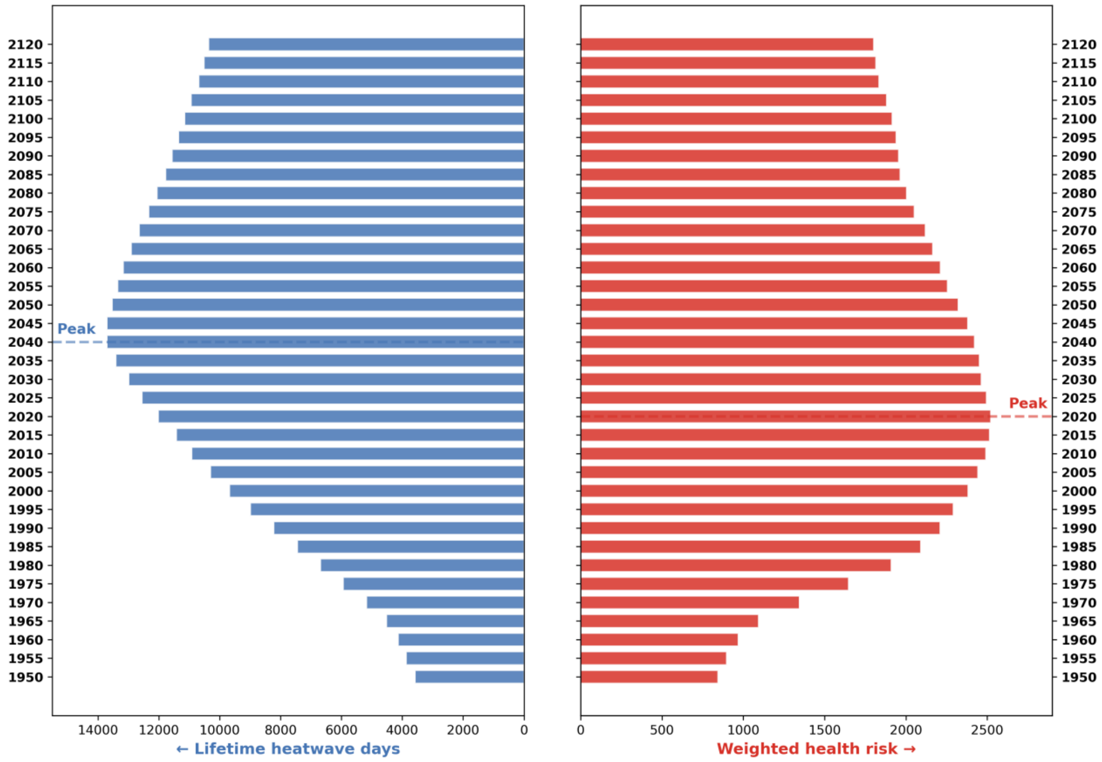

Supplementary Figure 15. Cohort profiles of lifetime heatwave exposure and health risk for Oceania. In Oceania, the peak of lifetime health risk (2020 cohort) precedes the peak of physical exposure (2040 cohort) by two decades.

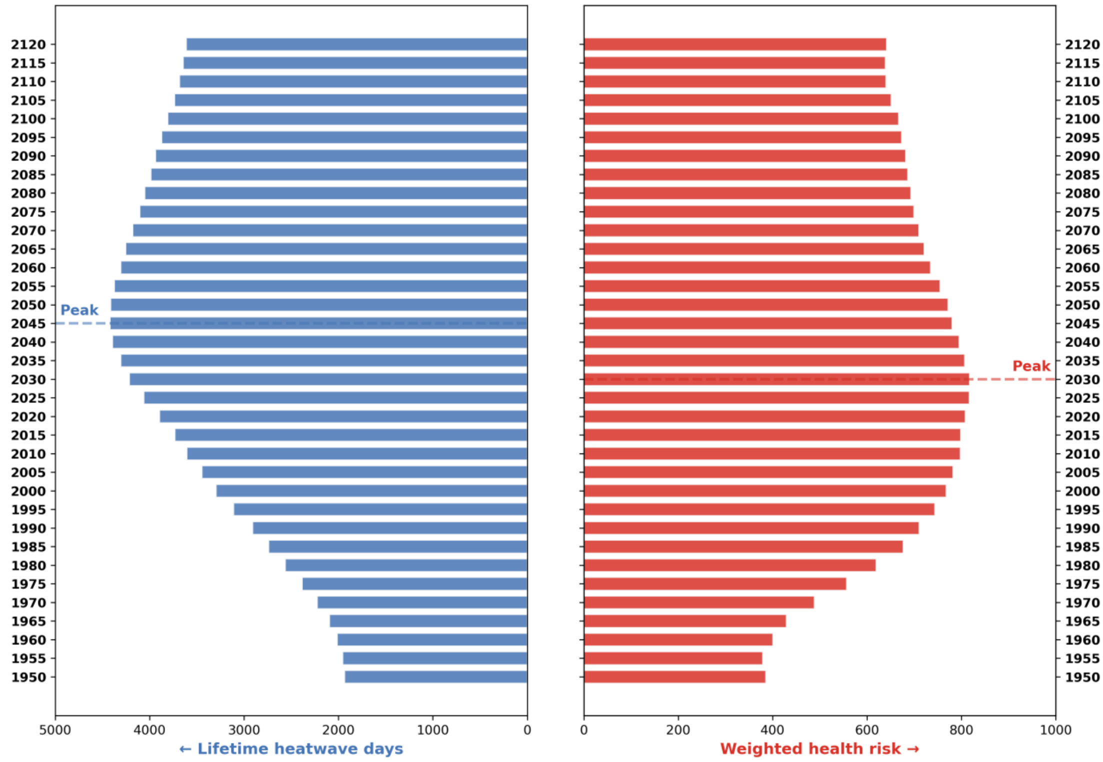

Supplementary Figure 16. Cohort profiles of lifetime heatwave exposure and health risk for South Asia. In South Asia, the generation with the highest lifetime heatwave exposure is born in 2045, but the highest health risk is observed in those born 15 years earlier, in 2030.

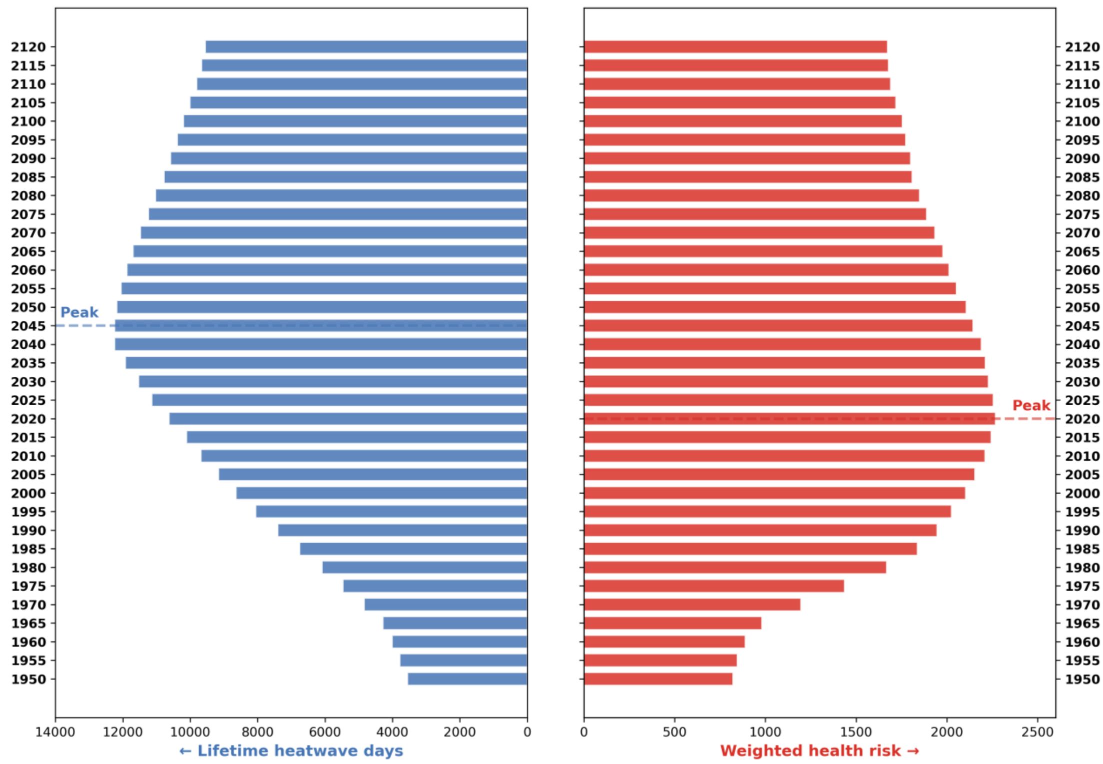

Supplementary Figure 17. Cohort profiles of lifetime heatwave exposure and health risk for Southeast Asia. In Southeast Asia, the generation with the highest lifetime heatwave exposure is born in 2045, but the highest health risk is observed in those born 25 years earlier, in 2020.

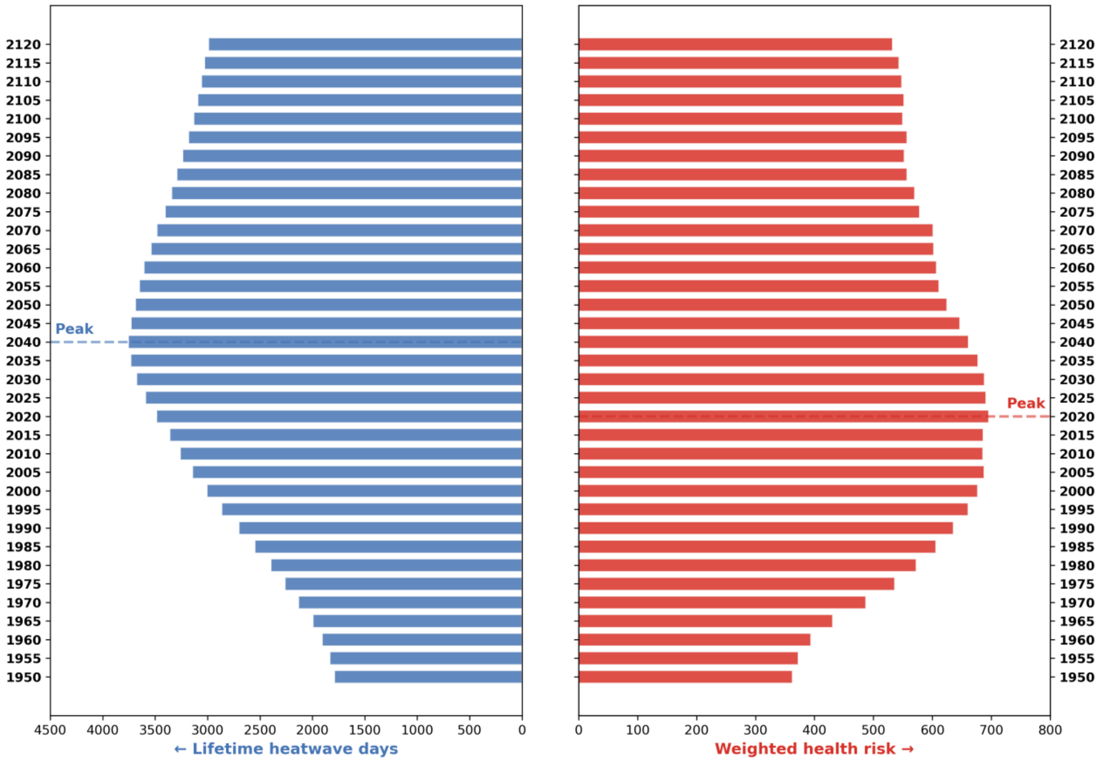

Supplementary Figure 18. Cohort profiles of lifetime heatwave exposure and health risk for Southern Latin America. In Southern Latin America, the peak of lifetime health risk (2020 cohort) precedes the peak of physical exposure (2040 cohort) by two decades.

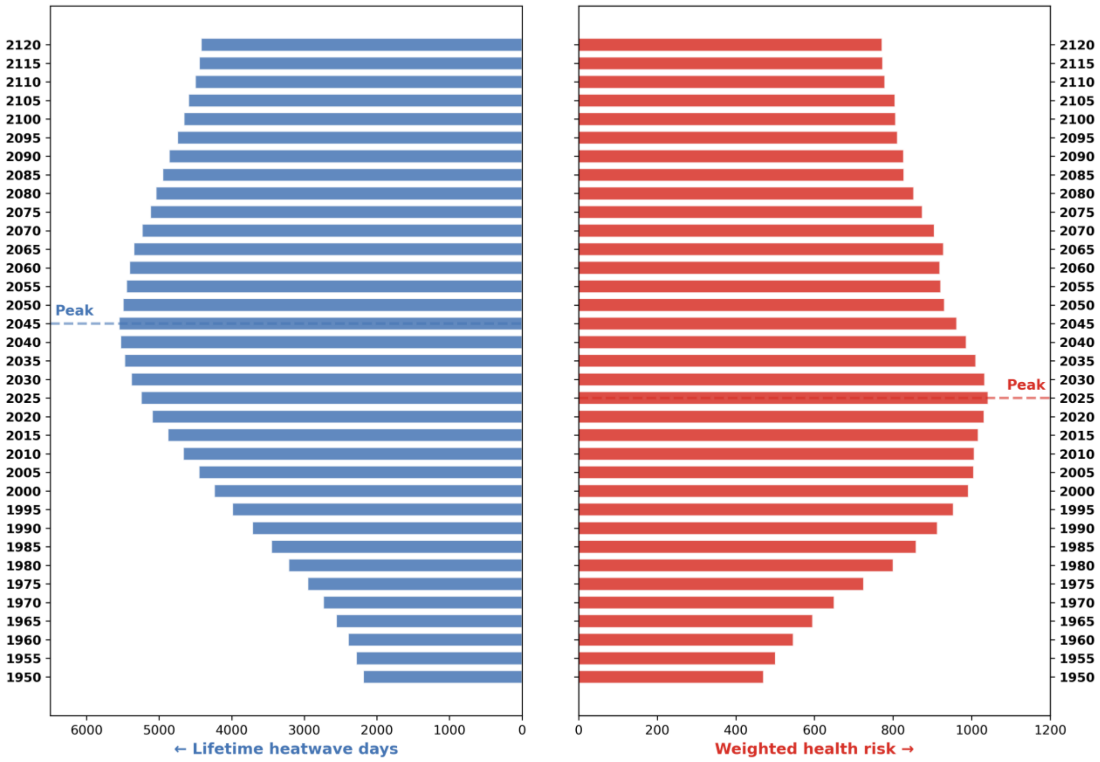

Supplementary Figure 19. Cohort profiles of lifetime heatwave exposure and health risk for Southern Sub-Saharan Africa. In Southern Sub-Saharan Africa, the peak of lifetime health risk (2025 cohort) precedes the peak of physical exposure (2045 cohort) by two decades.

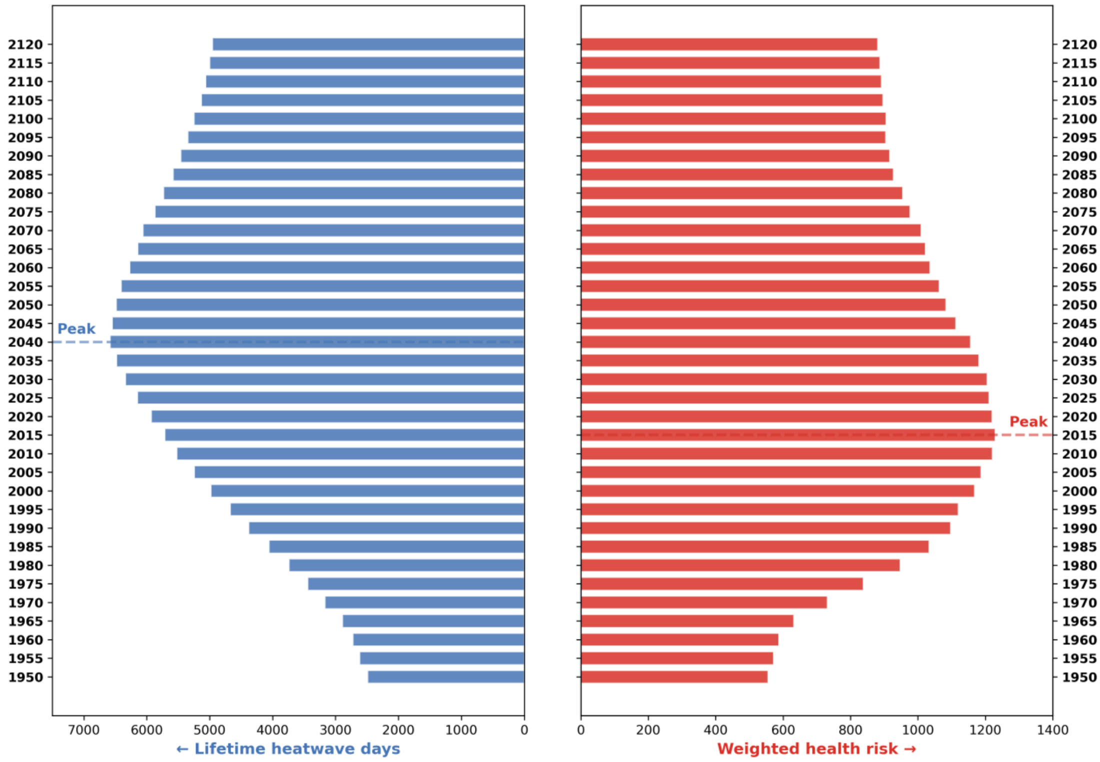

Supplementary Figure 20. Cohort profiles of lifetime heatwave exposure and health risk for Tropical Latin America. In Tropical Latin America, the generation with the highest lifetime heatwave exposure is born in 2040, but the highest health risk is observed in those born 25 years earlier, in 2015.

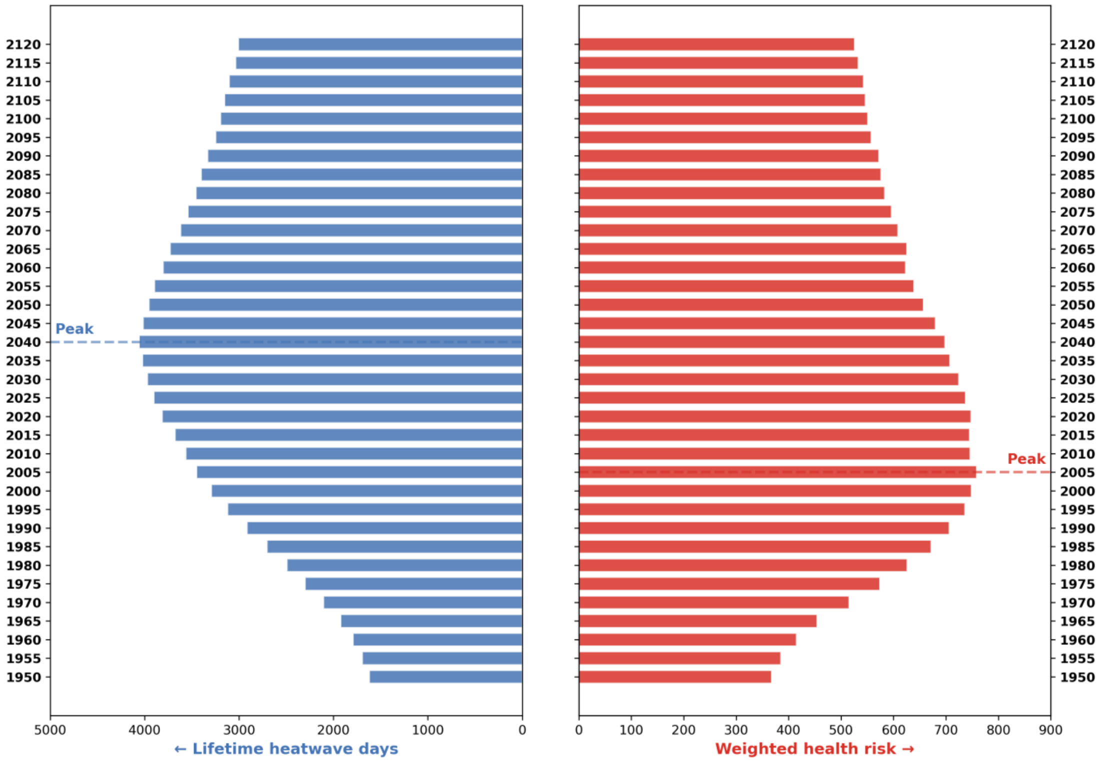

Supplementary Figure 21. Cohort profiles of lifetime heatwave exposure and health risk for Western Europe. A pronounced mismatch is evident in Western Europe: while lifetime exposure peaks for the 2040 cohort, the cumulative health risk reaches its maximum 35 years earlier (2005 cohort), reflecting a significant lead time in risk accumulation.

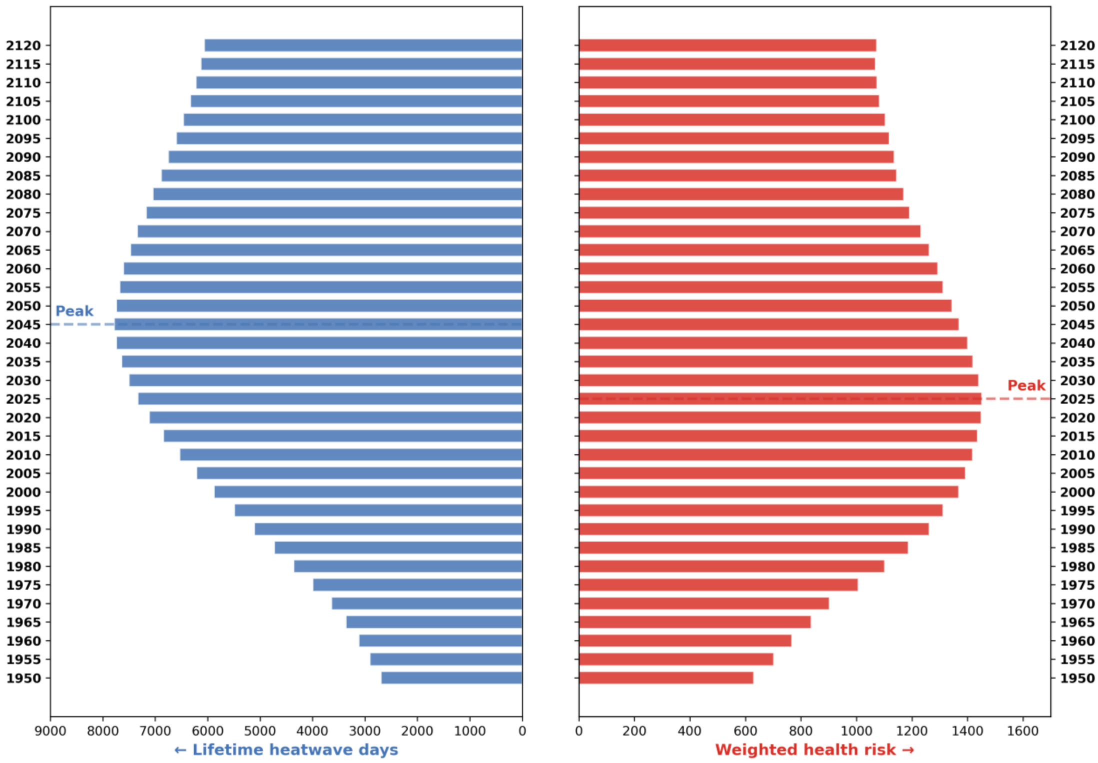

Supplementary Figure 22. Cohort profiles of lifetime heatwave exposure and health risk for

Western Sub-Saharan Africa. In Western Sub-Saharan Africa, the peak of lifetime health risk (2025 cohort) precedes the peak of physical exposure (2045 cohort) by two decades.